Temperature-Responsive One-Dimensional Nanogels Formed by the Cross-Linker-Aided Single Particle Nanofabrication Technique

Masaaki Omichi,[†,||] Hiromi Marui,[†] Katsuyoshi Takano,[†] Satoshi Tsukuda,[‡] Masaki Sugimoto,[§] Susumu Kuwabata,[†] and Shu Seki*,[†]

[†]Department of Applied Chemistry, Graduate School of Engineering, Osaka University, 2-1 Yamada-oka, Suita 565-0871, Japan
[‡]Institute of Multidisciplinary Research for Advanced Materials, Tohoku University, 2-1-1 Katahira, Aoba-ku, Sendai 980-8577, Japan
[§]Japan Atomic Energy Agency, Takasaki Advanced Radiation Research Institute, 1233 Watanuki-machi Takasaki, Gunma 370-1292, Japan

Ⓢ *Supporting Information*

ABSTRACT: A single particle nanofabrication technique was successfully applied to the fabrication of homogeneous poly(*N*-isopropylacrylamide) (PNIPAAm) 1D nanogels over a large area, using *N,N'*-methylene-bis-acrylamide (MBAAm) as a cross-linker. The PNIPAAm 1D nanogels with high aspect ratio over 130 were formed uniformly on the substrate, and the mechanical strength and the length of the 1D nanogels can be easily controlled by adjusting the MBAAm content. The 1D nanogels were transformed from the non-aggregated to aggregated forms over a lower critical solution temperature (LCST) of approximately 32 °C in water. Precise trace of the temperature induced change in the size of the 1D nanogel was well interpreted by the coil-to-globule transition of PNIPAAm, which was clearly visualized in the present study. This is the first report of uniform shape change for a 1D nanogel by external stimulus over a large area.

KEYWORDS: nanogel, single particle nanofabrication technique, temperature-responsive, cross-linker, poly(N-isopropylacrylamide), N,N'-methylene-bis-acrylamide
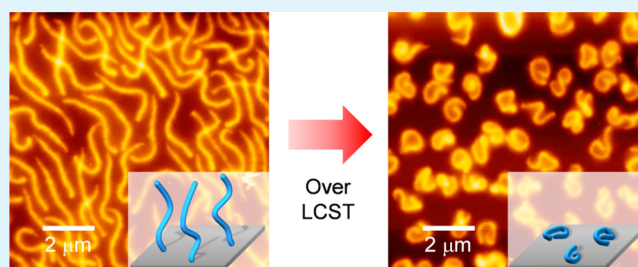
INTRODUCTION

Living organisms include various elements of highly organized biological structures at the nano- and microscales over a large area. Regular nano- and microstructures of biological materials exhibit properties such as superhydrophobicity, reversible adhesion, structural coloration, antireflection, sensory activity, and actuation.[1−6] There have been many attempts to fabricate controlled and homogeneous structures over a large area to mimic biological materials, and various controlled and homogeneous nano- and microstructures have been reported.[7−17] However, there have been few reports regarding nanostructures with high aspect ratios and large areas, because nanostructures are generally fragile, and consequently, the methods for fabrication are limited.[14]

We have recently proposed a method for the fabrication of uniformly sized nanowires over a large area using a single particle nanofabrication technique (SPNT).[18−22] High-energy charged particles induce a non-homogeneous, cross-linking reaction in nanometer-scale cylindrical areas of the polymer films along their trajectories. The development of irradiated samples using good solvents to remove the non-cross-linked polymer afforded nanowires. This is an excellent method for the fabrication of homogeneous nanowires with controlled length; however, it is only applicable to polymers in which the

cross-linking reaction is effectively induced by high-energy charged particles.

Poly(*N*-isopropylacrylamide) (PNIPAAm) is a thermoresponsive polymer with a lower critical solution temperature (LCST) of approximately 32 °C in water.[23,24] At room temperature, PNIPAAm absorbs water, which results in swelling of the polymer and transformation to a hydrophilic state, whereas at temperatures higher than the LCST, PNIPAAm shrinks and transforms to a hydrophobic state. This is also indicative that PNIPAAm 1D nanogels will be thermoresponsive nanoactuators. As a sophisticated nanoactuator system, myosin−actin complexes have been well-developed; myosin is a motor protein, bound into actin filaments, walking unidirectionally along the filament.[25] Myosin−actin complexes contribute to muscle contraction and have been much attractive as nanoactuators for several decades.[26] However, the cross-linking reaction does not occur so effectively in PNIPAAm by irradiation with high-energy charged particles. Therefore, the addition of the *N,N'*-methylene-bis-acrylamide (MBAAm) cross-linker to PNIPAAm is expected to increase the cross-linking efficiency under

irradiation and control of the cross-linking density to maintain nanostructures. Here, we report the fabrication of large area, highly organized one-dimensional (1D) PNIPAAm nanogels with sufficient mechanical strength using MBAAm as a cross-linker.

RESULTS AND DISCUSSION

A 1-μm-thick PNIPAAm-MBAAm spin-coated film (PNIPAAm/MBAAm = 100/20) was irradiated with a 490 MeV $^{192}Os^{30+}$ ion beam at a fluence of 1.0×10^8 ions/cm^2. The irradiated film was developed with isopropanol, which has low surface tension, because nano- and microstructures with high aspect ratios are easily destroyed by high-surface-tension solvents, such as water, during the development process.[27,28] After drying, the surface of the irradiated film was observed by atomic force microscopy (AFM). The AFM image suggested that 1D nanogels with cross-linked structures were successfully fabricated by ion beam irradiation (Figure 1). The range (>30
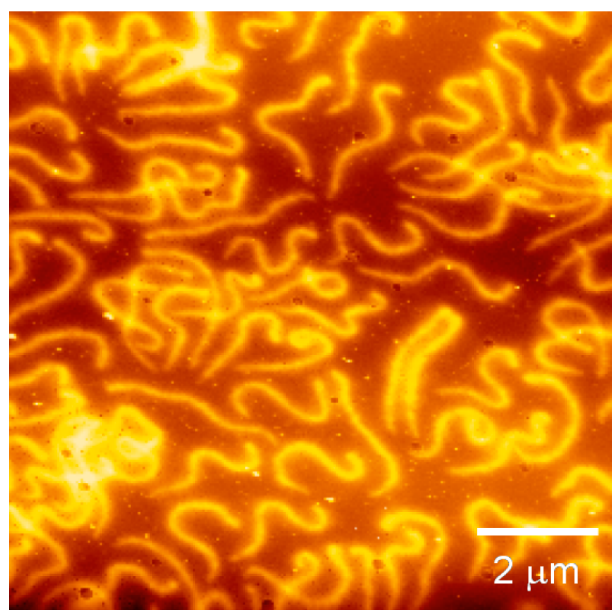

Figure 1. AFM image of the PNIPAAm 1D nanogels formed by irradiation of a 1-μm-thick PNIPAAm-MBAAm spin-coated film (PNIPAAm/MBAAm = 100/20) with a 490 MeV $^{192}Os^{30+}$ ion beam at a fluence of 1.0×10^8 ions/cm^2.

μm) of the incident particles was far longer than the thickness of PNIPAAm-MBAAm film, and the particles were passing through the polymer layer, and stopped deeply into the Si substrate. Because of the mismatch of the materials density of the PNIPAAm-MBAAm ($\rho \approx 0.9$ g/cm^3) and Si ($\rho = 2.3$ g/cm^3), back scattering of the secondary electrons knocked-out by incident particles causes proximity effects at the polymer/Si interface, leading to the accumulation of reactive intermediates at the interface. This is the case giving the tight binding of the nanogels onto the substrate surfaces via covalent bonds.

The ATR-FTIR spectrum of the PNIPAAm 1D nanogel was compared with those of PNIPAAm powder and PNIPAAm-MBAAm gel produced from PNIPAAm and MBAAm by the radical cross-linking reaction under UV irradiation to examine the chemical change induced by heavy ion irradiation (Figure 2). The IR peaks at 1630 and 1525 cm^{-1} were assigned to the amide group, and those at 1385 and 1365 cm^{-1} were assigned
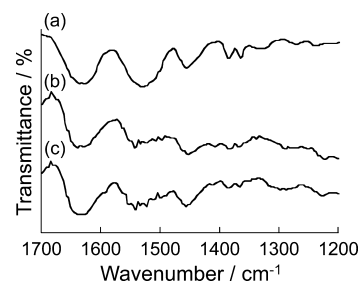

Figure 2. ATR-FTIR spectra of (a) PNIPAAm powder, (b) PNIPAAm 1D nanogels formed by ion beam irradiation, and (c) PNIPAAm-MBAAm gel formed by UV irradiation.

to the isopropyl group. These results indicate that the temperature-responsive sites of PNIPAAm were not changed by heavy ion irradiation. The IR spectrum of the ion beam-irradiated PNIPAAm 1D nanogel was very similar to that of the PNIPAAm-MBAAm gel produced under UV irradiation. Therefore, it is most likely that heavy ion irradiation generated radicals, so that the radical cross-linking reaction of PNIPAAm and MBAAm occurred in a similar way to that for UV irradiation.

To examine the homogeneity of PNIPAAm 1D nanogels formed from a 1-μm-thick PNIPAAm-MBAAm film, the lengths of the PNIPAAm 1D nanogels were estimated from AFM observation, and the length distribution is shown in Figure 3. There was little variability in the length among the PNIPAAm 1D nanogels and the average length was 2.58 μm, which was not same as the film thickness (1 μm).
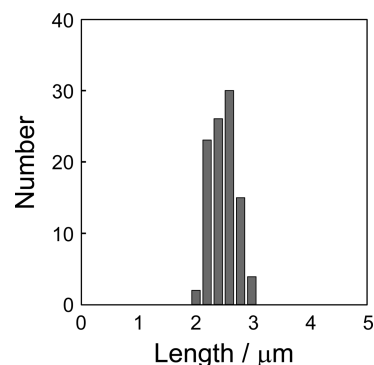

Figure 3. Length distribution of the PNIPAAm 1D nanogels ($n = 100$) formed from a 1-μm-thick PNIPAAm-MBAAm nanogel film.

The discrepancy in length must be attributable to swelling of the PNIPAAm 1D nanogels in isopropanol, where the lengths in the swollen state were maintained due to the strong interaction between the PNIPAAm 1D nanogels and the Si wafer during the drying process. The result indicates that highly homogeneous PNIPAAm 1D nanogels were successfully fabricated. The diameter of the 1D nanogels was approximately 40 nm, which is compatible with the size of motor proteins such as actin-myosin (ca. 20−30 nm).[29]

The effects of the MBAAm content on the length and the radius of the PNIPAAm 1D nanogels were examined using AFM (Figure 4a−c). The length of the 1D nanogels decreased with increasing MBAAm content, while the radius increased with the MBAAm content (Figure 4d). It is reasonable that the length and the radius changed inversely. For a lower MBAAm content, the length was long and showed rather wide variability.
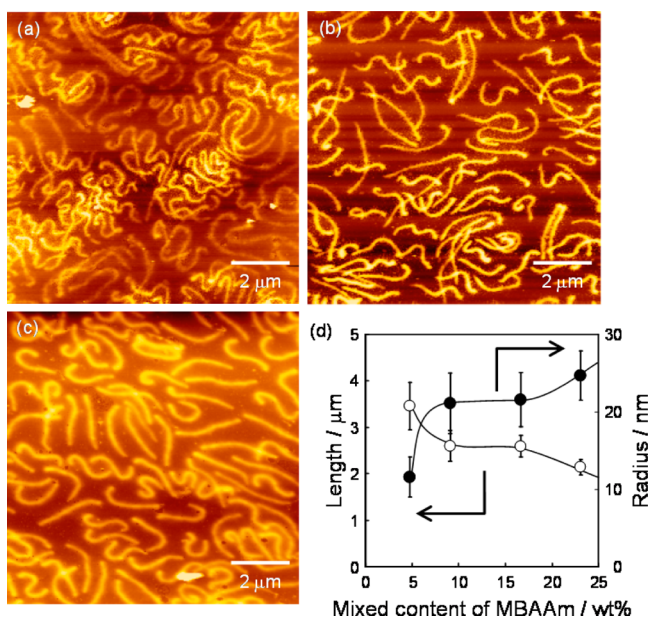
Figure 4. AFM images of the PNIPAAm 1D nanogels formed by 490 MeV ^{192}Os^{30+} ion beam irradiation (1.0×10^8 ions/cm^2 fluence) of 1-μm-thick PNIPAAm-MBAAm spin-coated films with MBAAm contents (PNIPAAm/MBAAm) of (a) 100/5, (b) 100/10, and (c) 100/30. (d) Dependence of the length and radius of the nanogel on the MBAAm content of the film.

It is likely that these 1D nanogels broke in several parts because of low mechanical strength caused by low degree of cross-linking and were removed during the development process. For a higher MBAAm content, the length was short and the variability was narrow due to higher mechanical strength as a result of a higher degree of cross-linking. In general, the degree of cross-linking increased with increasing the MBAAm content of the PNIPAAm gels.[30] These results indicate that the mechanical strength of the 1D nanogels can be controlled by adjusting the MBAAm content.

The relationship between the thickness of the PNIPAAm-MBAAm spin-coated film and the length of the PNIPAAm 1D nanogels formed by ion beam irradiation was examined for a PNIPAAm/MBAAm (= 100/20) film. The nanogel length increased in direct proportion to the film thickness (coefficient of variation $R^2 = 0.989$) (Figure 5a), which confirms that homogeneous cross-linking occurred in the film, even if the film thickness increased. For a 2-μm-thick film, the aspect ratio of the PNIPAAm 1D nanogels formed was reached up to 130
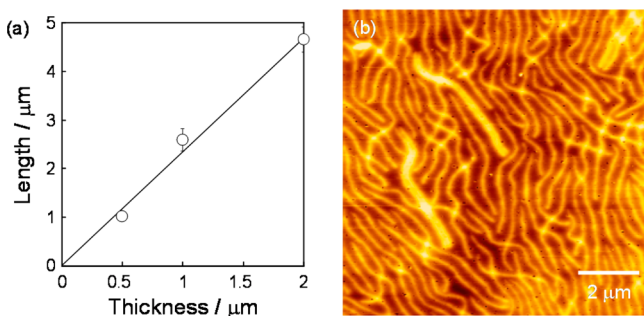

Figure 5. (a) Length of the 1D nanogels ($n = 30$) as a function of the PNIPAAm-MBAAm spin-coated film thickness. (b) AFM image of high aspect ratio 1D nanogels (length:radius = 130:1).

(Figure 5b), where the nanogels formed from the 0.5- and 1-μm films shows the aspect ratio of 28 and 75, respectively.

The linear correlation between the aspect ratio and the initial film thickness also supports the homogeneous distribution of cross-links along the major axis of 1D nanogels, leading to negligible change in the diameter at any cross sections of the nanogels. Following equation was proposed to give appropriate theoretical estimate for the diameter ($2r$) of 1D nanogels produced by cross-linking reactions induced by high energy single particle releasing its energy along the trajectory with the averaged energy deposition of linear energy transfer (LET, eV nm^{-1})[31,32]

$$r^2 = \frac{LETTG(x)mN}{400\pi\rho A}\left[\ln\left(\frac{e^{1/2}r_p}{r_c}\right)\right]^{-1} \tag{1}$$

where A is Avogadro's number, e is Napier's constant, m is the mass of a monomer unit, ρ (g/nm^3) is the density of the polymer, N is the degree of polymerization, $G(x)$ $(100 \text{ eV})^{-1}$ is number of cross-links induced by a radiation-deposited energy of 100 eV, r_c and r_p are the radii of the core and penumbra areas, defined from the equipartition theorem of collisions of charged particles with matter.[21,33] Assuming spatial homogeneous distribution of MBAAm cross-linker, the estimate of diameter derived from eq 1 depends only on the value of LET of the incident particle. The value of LET is calculated as 12000 eV nm^{-1} for 490 MeV ^{192}Os^{30+} in a PNIPAAm/MBAAm (= 100/20) film, and the value is almost constant (less than 1% decrease) over the trajectories of incident particle as long as 4 μm. This is the case giving homogeneous cross-linking in the PNIPAAm 1D nanogels and linear correlation between aspect ratio and the initial film thickness. The cross-linking efficiency of $G(x)$ is also derived from eq 1 from observed values of r, estimated as $G(x) = 0.45$, 1.6, 1.7, and 2.8 $(100 \text{ eV})^{-1}$ for the film with varying contents of MBAAm (PNIPAAm/MBAAm) at 100/5, 100/10, 100/20, and 100/30, respectively. The value of $G(x)$ has been reported to depend strongly on the LET values of the incident particle, because radical coupling and/or the other second order reactions often control the cross-linking reaction in polymer materials without cross-linkers.[34,35] In the present case, primary the cross-links were introduced by pseudofirst order reactions via MBAAm cross-linker molecules, giving the less dependence on the LET values.

In spite of identical set of a polymer and a cross-linker, the efficiency dramatically increases with an increase in mixed contents of MBAAm, leading to the higher density of cross-links in the PNIPAAm 1D nanogels and mechanical strength. The nanogel with a low cross-linking density and a high aspect ratio has poor mechanical strength; however, by adjusting the film thickness and the MBAAm content, we can fabricate PNIPAAm 1D nanogels with any aspect ratio and adequate mechanical strength.

The form of the 1D nanogels incubated in water at various temperatures was examined (Figure 6a–c). The 1D nanogels transformed from the non-aggregated form to the aggregated form with increasing temperature (Figure 6d). The transformation was likely to be due to dehydration of the 1D nanogels. The morphologies slightly changed over 40 °C (Figure 6b,c), suggesting that the dehydration of the 1D PNIPAAm nanogels is still in progress over LCST.

Panels a and b in Figure 7 show the length and radius distributions of 1D nano gels incubated in water at 25 °C, 40
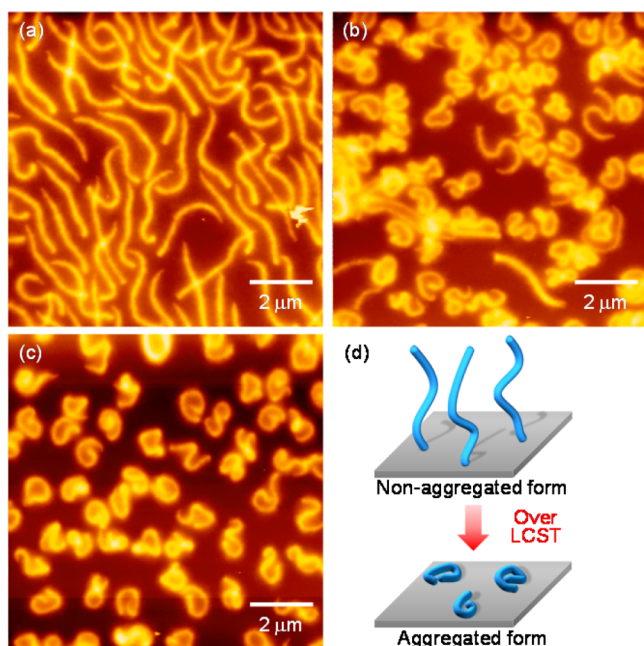
Figure 6. AFM images of PNIPAAm 1D nanogels treated in water at (a) 25 °C, (b) 40 °C, and (c) 50 °C. The 1D nanogels were formed by irradiation of a 1-μm-thick PNIPAAm/MBAAm (= 100/20) spin-coated film with a 490 MeV $^{192}Os^{30+}$ ion beam (1.0×10^8 ions/cm^2 fluence). (d) Schematic image showing the transformation of PNIPAAm 1D nanogel from nonaggregated to aggregated forms in response to increasing temperature.
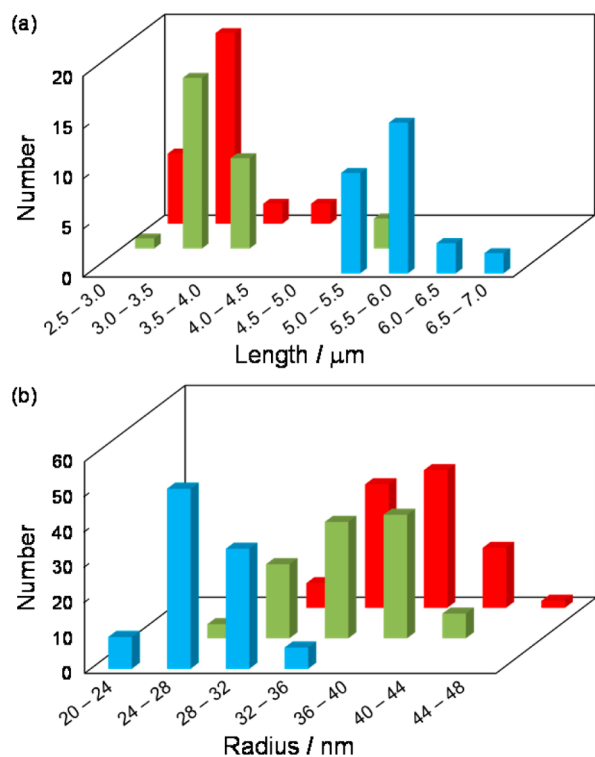

Figure 7. (a) Length ($n = 30$) and (b) radius distributions ($n = 100$) of the PNIPAAm 1D nanogels at 25 °C (blue), 40 °C (green), and 50 °C (red).

°C, and 50 °C. The average lengths at 25 °C, 40 °C, and 50 °C were 5.72 ± 0.40, 3.56 ± 0.65, and 3.25 ± 0.35 μm, respectively. Swollen and shrunken states were observed at 25

°C and 50 °C, respectively, and at 40 °C, both states were observed. The variation in length for the swollen state at 25 °C (0.40 μm) and the shrunken state at 50 °C (0.35 μm) could be attributed to the variation in the gyradius with the LCST. The results are compatible with previous reports regarding the coil-to-globule transition of PNIPAAm.[23,24] The average radii at 25 °C, 40 °C, and 50 °C were 27.6 ± 2.7, 34.8 ± 3.5, 36.8 ± 3.4 nm. The average volumes at 25 °C, 40 °C, and 50 °C were calculated from the length and radius to be 1.36×10^7, 1.35×10^7, and 1.38×10^7 nm^3, respectively. The similar volumes of the 1D nanogels suggest that the radius of the 1D nanogels does not reflect the swollen/shrunken state, in contrast to the 1D nanogel length, and this is why the variation in the radius at 50 °C was larger than that at 25 °C. To the best of our knowledge, this is the first report to show that the shape of each 1D nanogel is uniformly changed by external stimulus over a large area. Thus, an assembly of PNIPAAm 1D nanogels in water could be expected to act as a nanoactuator. Solvent swelling ratio of PNIPAAm-based gel systems has been reported to depend not only on the temperature but also on ionic strength.[36] The pH-responsive properties of the present nanogel systems were also examined, showing the lower swelling ratio in the acidic conditions (see Figure S1 in the Supporting Information).

Contact angle measurement is a useful technique to evaluate the hydrophobicity of a surface. The contact angles of the surface of 1D nanogels (PNIPAAm/MBAAm = 100/20) on a Si wafer were measured at different temperatures. The contact angle of the PNIPAAm 1D nanogel surface at 40 °C was larger than that at 25 °C (Figure 8). The change in contact angle after
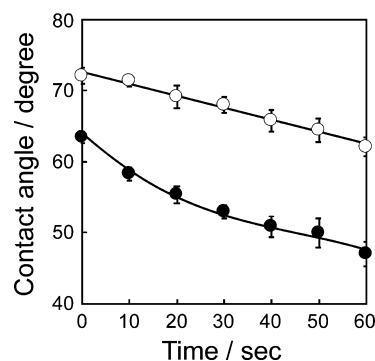

Figure 8. Contact angles of the PNIPAAm 1D nanogel surface at 25 °C (●) and 40 °C (○).

1 min at 25 °C was larger than that at 40 °C. These results suggest that the PNIPAAm 1D nanogels absorb water, which results in a hydrophilic surface under LCST. However, at temperatures over LCST, the nanogels do not readily absorb water, and the surface remains hydrophobic. Interestingly, time course of the contact angle at 25 °C exhibited curve, although that at 40 °C exhibited straight line. This fact might be attributable to difference in water absorption of the 1D nanogels between 25 °C and 40 °C. At 25 °C, the contact angle dramatically decreased because of high water absorption of the 1D nanogels, and variation of contact angle was gradually decreased. On the other hand, at 40 °C, low water absorption of the 1D nanogels caused slight decrease of contact angle. Each PNIPAAm 1D nanogel has little effect on the surface properties; however, an assembly of the 1D nanogels would cause a macroscopic change in the surface properties.

■ CONCLUSION

PNIPAAm 1D nanogels were successfully fabricated using the SPNT with a cross-linker. PNIPAAm 1D nanogels with diameters from 20 to 40 nm were obtained, which is compatible with the size of motor proteins, such as the actin-myosin complex. This fabrication method can be used to control the length and cross-linking density of the 1D nanogels. The 1D nanogels swell uniformly at temperatures under LCST and shrink over LCST. The 1D nanogels have sufficient mechanical strength not to break even in water. To date, the SPNT has been applied only for the fabrication of polymers with high cross-linking efficiency. Application of the SPNT with combination of a cross-linker and a functional polymer, such as a biopolymer, is expected to be very effective for the fabrication of various functional 1D nanogels and should contribute to the development of nanoactuators and highly sensitive sensory devices.

■ EXPERIMENTAL SECTION

Materials. Poly(N-isopropylacrylamide) (M_w = 20 000−25 000 g/mol) and N,N′-methylene-bis-acrylamide were purchased from Sigma-Aldrich Corporation (St. Louis, USA). Methanol was purchased from Wako Pure Chemical Industries, Ltd. (Osaka, Japan). Isopropanol was purchased from Kishida Chemical Corporation, Ltd. (Osaka, Japan).

Fabrication of PNIPAAm 1D Nanogels on Si Wafers. PNIPAAm-MBAAm blend films were prepared on Si wafers (1.5 × 1.5 cm^2) by spin-casting PNIPAAm with variable MBAAm contents (PNIPAAm/MBAAm = 100/0, 100/5, 100/10, 100/20, and 100/30) in methanol at 2000 rpm for 1 min. The thickness of the films was adjusted to 0.5, 1, and 2 μm, which was confirmed using a stylus surface profiler (Dektak 150, Ulvac, Inc., Japan). The spin-cast nanogel films were irradiated in a vacuum chamber (<1 × 10^{-4} Pa) with a 490 MeV ^{192}Os^{30+} ion beam from the cyclotron accelerator at Takasaki Advanced Radiation Research Institute, Japan Atomic Research Agency. The fluence of the incident ions varied from 1 × 10^8 to 1 × 10^9 ions/cm^2. After irradiation, the samples were developed in isopropanol for 30 min and dried at room temperature overnight. The irradiated part of the film was insoluble in isopropanol.

AFM Observation of 1D PNIPAAm Nanogels. The PNIPAAm 1D nanogels on Si wafer were observed by atomic force microscopy (AFM). AFM images were obtained in air and at room temperature using a microscope (SPA-400, SII, Japan) operated in the tapping mode. The radius of the cross-section (r) in any given nanowire was estimated from the following equation

$$r = \sqrt{r_1 r_2}$$

where r_1 and r_2 are the half-width and half-height at half-maximum from the AFM trace of the cross-section, respectively.

ATR-FTIR Observation of the PNIPAAm 1D Nanogels. Attenuated total reflectance-Fourier-transform infrared (FTIR-ATR; Spectrum 100 FT-IR, Perkin-Elmer Japan) spectra of the PNIPAAm 1D nanogels formed by ion beam irradiation of a 1-μm-thick PNIPAAm-MBAAm spin-coated film (PNIPAAm/MBAAm = 100/20) with a fluence of 1.0 × 10^9 ions/cm^2, as well as those of the PNIPAAm powder and PNIPAAm-MBAAm gel formed by UV irradiation of a 1-μm-thick PNIPAAm-MBAAm spin-coated film (PNIPAAm/MBAAm = 100/20) were measured. The interferograms were coded 16 times and Fourier-transformed at a resolution of 4 cm^{-1}.

Temperature-Responsivity of PNIPAAm 1D Nanogels by AFM Observation. PNIPAAm 1D nanogels formed on a Si wafer by ion beam irradiation of a 1-μm-thick PNIPAAm-MBAAm spin-coated film (PNIPAAm/MBAAm = 100/20) with a fluence of 1.0 × 10^8 ions/cm^2 were incubated in water at 25 °C, 40 °C, and 50 °C for 10 min. The PNIPAAm 1D nanogels were then dried at the same respective temperatures for 1 h prior to AFM observation.

Static Contact Angle Measurements of the PNIPAAm 1D Nanogels on Si Wafer. The static contact angle of PNIPAAm 1D nanogel surfaces (1-μm-thick PNIPAAm/MBAAm = 100/20 spin-coated film on Si wafer irradiated at a fluence of 1.0 × 10^9 ions/cm^2) were measured at 25 °C and 40 °C for 1 min using a contact angle meter (DropMaster 500, Kyowa InterFACE Science Co., Ltd., Japan). A 0.5 μL water droplet was placed on a sample and the average of three identical measurements was taken.

■ ASSOCIATED CONTENT

⑤ Supporting Information

Figures showing morphological changes of PNIPAAm-based nanogels under a variety of pH conditions. This material is available free of charge via the Internet at http://pubs.acs.org.

■ AUTHOR INFORMATION

Corresponding Author

*Tel.: +81-6-6879-4587. Fax +81-6-6879-4588. E-mail: seki@chem.eng.osaka-u.ac.jp.

Present Address

‖Center for Collaborative Research, Anan National College of Technology, 265 Aoki Minobayashi, Anan, Tokushima 774−0017, Japan Tel/Fax, +81−884−23−7294

Notes

The authors declare no competing financial interest.

■ ACKNOWLEDGMENTS

■ REFERENCES

(1) Barthlott, W.; Neinhuis, C. Planta 1997, 202, 1−8.
(2) Autumn, K.; Liang, Y. A.; Hsieh, S. T.; Zesch, W.; Chan, W. P.; Kenny, T. W.; Fearing, R.; Full, R. J. Nature 2000, 405, 681−685.
(3) Ghiradella, H.; Aneshansley, D.; Eisner, T.; Silberglied, R. E.; Hinton, H. E. Science 1972, 178, 1214−1217.
(4) Clapham, P. B.; Hutley, M. C. Nature 1973, 244, 281−282.
(5) Coombs, S. Auton. Robots 2001, 11, 255−261.
(6) Sleigh, M. A.; Blake, J. R.; Liron, N. Am. Rev. Respir. Dis. 1988, 137, 726−741.
(7) Chen, W.; Fadeev, A. Y.; Hsieh, M. C.; Oner, D.; Youngblood, J.; McCarthy, T. J. Langmuir 1999, 15, 3395−3399.
(8) Feng, L.; Li, S.; Li, Y.; Li, H.; Zhang, L.; Zhai, J.; Song, Y.; Liu, B.; Jiang, L.; Zhu, D. Adv. Mater. 2002, 14, 1857−1860.
(9) Yabu, H.; Hirai, Y.; Kojima, M.; Shimomura, M. Chem. Mater. 2009, 21, 1787−1789.
(10) Geim, A. K.; Dubonos, S. V.; Grigorieva, I. V.; Novoselov, K. S.; Zhukov, A. A.; Shapoval, S. Y. Nat. Mater. 2003, 2, 461−463.
(11) Sitti, M.; Fearing, R. S. J. Adhes. Sci. Technol. 2003, 17, 1055−1073.
(12) Gu, Z. Z.; Uetsuka, H.; Takahashi, K.; Nakajima, R.; Onishi, H.; Fujishima, A.; Sato, O. Angew. Chem., Int. Ed. 2003, 8, 894−897.
(13) Feng, L.; Zhang, Y.; Li, M.; Zheng, Y.; Shen, W.; Jiang, L. Langmuir 2010, 26, 14885−14888.
(14) Lalanne, P.; Morris, G. M. Nanotechnology 1997, 8, 53−56.
(15) Huang, Y. F.; Chattopadhyay, S.; Jen, Y. J.; Peng, C. Y.; Liu, T. A.; Hsu, Y. K.; Pan, C. L.; Lo, H. C.; Hsu, C. H.; Chang, Y. H.; Lee, C. S.; Chen, K. H.; Chen, L. C. Nat. Nanotechnol. 2007, 2, 770−774.

(16) Evans, B. A.; Shields, A. R.; Carroll, R. L.; Washburn, S.; Falvo, M. R.; Superfine, R. *Nano Lett.* **2007**, *7*, 1428−1434.

(17) den Toonder, J.; Bos, F.; Broer, D.; Filippini, L.; Gillies, M.; de Goede, J.; Mol, T.; Reijme, M.; Talen, W.; Wilderbeek, H.; Khatavkar, V.; Anderson, P. *Lab Chip* **2008**, *8*, 533−541.

(18) Seki, S.; Maeda, K.; Kunimi, Y.; Tagawa, S.; Yoshida, Y.; Kudoh, H.; Sugimoto, M.; Morita, Y.; Segchi, T.; Iwai, T.; Shibata, H.; Asai, K.; Ishigure, K. *J. Phys. Chem. B* **1999**, *103*, 3043−3048.

(19) Seki, S.; Maeda, K.; Tagawa, S.; Kudoh, H.; Sugimoto, M.; Morita, Y.; Shibata, H. *Adv. Mater.* **2001**, *13*, 1663−1665.

(20) Tsukuda, S.; Seki, S.; Tagawa, S.; Sugimoto, M.; Idesaki, A.; Tanaka, S.; Oshima, A. *J. Phys. Chem. B* **2004**, *108*, 3407−3409.

(21) Seki, S.; Tsukuda, S.; Maeda, K.; Matsui, Y.; Saeki, A.; Tagawa, S. *Phys. Rev. B* **2004**, *70*, 144203.

(22) Tsukuda, S.; Seki, S.; Sugimoto, M.; Tagawa, S. *Jpn. J. Appl. Phys.* **2005**, *44*, 5839−5842.

(23) Wu, C.; Wang, X. *Phys. Rev. Lett.* **1998**, *80*, 4092−4094.

(24) Wang, X.; Qiu, X.; Wu, C. *Macromolecules* **1998**, *31*, 2972−2976.

(25) Bagshaw, C. R. *Essays Biochem.* **2000**, *35*, 19−31.

(26) Kinbara, K.; Aida, T. *Chem. Rev.* **2005**, *105*, 1377−1400.

(27) Tanaka, T.; Morigami, M.; Atoda, N. *Jpn. J. Appl. Phys.* **1993**, *32*, 6059−6064.

(28) del Campo, A.; Arzt, E. *Chem. Rev.* **2008**, *108*, 911−945.

(29) Kodera, N.; Yamamoto, D.; Ishikawa, R.; Ando, T. *Nature* **2010**, *468*, 72−76.

(30) Senff, H.; Richteing, W. *Colloid Polym. Sci.* **2000**, *278*, 830−840.

(31) Seki, S.; Tsukuda, S.; Maeda, K.; Tagawa, S.; Shibata, H.; Sugimoto, M.; Jimbo, K.; Hashitomi, I.; Kohyama, A. *Macromolecules* **2005**, *38*, 10164−10170.

(32) Seki, S.; Tsukuda, S.; Tagawa, S.; Sugimoto, M. *Macromolecules* **2006**, *39*, 7446−7450.

(33) Magee, J. L.; Chattarjee, A.; *Kinetics of Nonhomogenious Processes*; Freeman, G. R., Ed.; John Wiley & Sons: New York, 1987; Chapter 4, p171.

(34) Seki, S.; Shibata, H.; Ban, H.; Ishigure, K.; Tagawa, S. *Radiat. Phys. Chem.* **1996**, *48*, 539−544.

(35) Seki, S.; Tagawa, S. *Polym. J.* **2007**, *39*, 277−293.

(36) Daly, E.; Saunders, B. R. *Phys. Chem. Chem. Phys.* **2000**, *2*, 3187−3193.